Indo. J. Chem., 2014, 14 (3), 253 - 261

253

THE EFFECT OF CARAMELIZATION AND CARBONIZATION TEMPERATURES TOWARD STRUCTURAL PROPERTIES OF MESOPOROUS CARBON FROM FRUCTOSE WITH ZINC BOROSILICATE ACTIVATOR

Tutik Setianingsih[1,2,*], Indriana Kartini[2], and Yateman Arryanto[2]

[1]Department of Chemistry, Faculty of Mathematics and Natural Sciences, Brawijaya University,
Jl. Veteran Malang 65145, Indonesia

[2]Department of Chemistry, Faculty of Mathematics and Natural Sciences, Universitas Gadjah Mada,
Sekip Utara Yogyakarta 55281, Indonesia

ABSTRACT

Mesoporous carbon was prepared from fructose using zinc borosilicate (ZBS) activator. The synthesis involves caramelization and carbonization processes. The effect of both process temperature toward porosity and functional group of carbon surface are investigated in this research. The caramelization was conducted hydrothermally at 85 and 100 °C, followed by thermally 130 °C. The carbonization was conducted at various temperatures (450–750 °C). The carbon-ZBS composite were washed by using HF 48% solution, 1M HCl solution, and aquadest respectively to remove ZBS from the carbon. The carbon products were characterized with nitrogen gas adsorption-desorption method, FTIR spectrophotometry, X-ray diffraction, and Transmission Electron Microscopy. The highest mesopore characteristics is achieved at 100 °C (caramelization) and 450 °C (carbonization), including V_{meso} about 2.21 cm³/g (pore cage) and 2.32 cm³/g (pore window) with pore uniformity centered at 300 Å (pore cage) and 200 Å (pore window), containing the surface functional groups of C=O and OH, degree of graphitization about 57% and aromaticity fraction about 0.68.

Keywords: mesoporous carbon; zinc borosilicate; fructose; temperature

ABSTRAK

Karbon mesopori telah dipreparasi dari fruktosa dengan menggunakan seng borosilikat (ZBS) aktivator. Sintesis melibatkan proses karamelisasi dan karbonisasi. Pengaruh temperatur kedua proses terhadap porositas dan gugus fungsi permukaan karbon dikaji dalam penelitian ini. Karamelisasi dilakukan secara hidrotermal pada 85 dan 100 °C, diikuti secara termal pada 130 °C. Karbonisasi dilakukan pada berbagai temperatur (450-750 °C). Karbon produk dicuci dengan larutan HF 48%, larutan HCl 1M, dan akuades secara berurutan untuk menghilangkan ZBS dari karbon. Produk karbon dikarakterisasi dengan metode adsorpsi–desorpsi gas nitrogen, spektrofotometri FTIR, difraksi sinar X, dan mikroskopi transmisi elektron. Karakterisasi mesopori tertinggi dicapai pada 100 °C (karamelisasi) dan 450 °C (karbonisasi), meliputi V_{meso} 2,21 cm³/g (rongga pori) and 2,32 cm³/g (jendela pori) dengan keseragaman pori terpusat pada ukuran pori 300 Å (rongga pori) and 200 Å (jendela pori), yang mengandung gugus permukaan C=O dan OH, derajat grafitisasi ≈ 57% dan fraksi aromatisitas ≈ 0,68.

Kata Kunci: karbon mesopori; seng borosilikat; fruktosa; temperatur

INTRODUCTION

Mesoporous carbon (2-50 nm pore size) is an interesting material due to its properties and its potential applications. Chemically, the mesoporous carbon is resistant to acid and base [1]. Functional group of the carbon surface can be engineered by oxidation treatments [2]. The mesoporous carbon has various potential applications, including as adsorbent of large molecule [3]. Mesoporous volume and pore size distribution determine capacity of adsorption [4] and the equilibrium time of adsorption [3].

Some researchers reported that carbonization temperature gives influence toward surface's functional groups and porosity of the carbon. There is decrease of functional group amount by increase of carbonization temperature [5]. Connected to porosity, the influence is different for various activators or templates of the carbon. For example, NaOH, KOH, Na_2CO_3, K_2CO_3 activators [6] and silica template [7] improve mesoporous volume by temperature increase for range

* Corresponding author.
Email address : tutiksetia@ub.ac.id

more than 600 °C. Silica also increases pore uniformity by increase of temperature [8]. However, $ZnCl_2$ is a chemical activator which forms porosity well at low temperature not more than 600 °C [6,9-11]. The $ZnCl_2$ activator built the mesoporous carbon from fructose which has pore uniformity centered on 7 nm at 450 °C [11]. This low temperature is enough efficient, but the quality of pore makes the carbon ineffective for adsorption of large adsorbate, for example marine bacteria which has size of 30–60 nm [12] or virus hepatitis A which has size of 28–40 nm [13]. In other side, borosilicate is a pore template which physically forms uniformity at 30 nm and 23 nm, but needs enough high carbonization temperature, i.e. 900 °C [14].

Zinc borosilicate is a combination of activator–template in synthesis of mesoporous carbon from sugar. This ceramics can open a chance to produce carbon with pore uniformity centered on > 7 nm but lower carbonization temperature. Physically, ZBS can act as pore template in carbonization process, which controls pore size of the carbon. Chemically, the Zn^{2+} cation has the role as activator of pyrolysis which supports carbonization at low temperature. Another benefit is that precursors of zinc borosilicate such as silica gel, boric acid, and $ZnCl_2$ are also proton donors in the water [18-20], meaning that they can catalyze caramelization of sugar. The caramelization process produces caramel which has a role in carbonization to create pore wall of the carbon. Technically, ZBS ceramics contains crystal zinc silicate and zinc borate which involves hydrothermal and calcination processes in synthesis [15-17]. This is similar to caramelization and carbonization in synthesis of carbon from sugar as reported in previous research [11].

Caramel is a large substance which has molecular formula of $C_{125}H_{188}O_{80}$ and bitter taste [21]. In synthesis of carbon from sugar, some researches performed the caramelization before carbonization process at different temperature with different sugar, for example: at 85 °C with fructose [11], at 100 °C with sucrose [14], and at 100 °C with glucose [22]. In transformation of carbohydrate to 5-hydroximethylfurfural (HMF) by acid condition, fructose produce more HMF than sucrose and glucose [23]. HMF is intermediate of caramel in caramelization process [11] and indicator of caramelization reaction [24]. Temperature improves caramelization reaction kinetics of monosaccharide and disaccharide [25].

In this research, mesoporous carbon is synthesized from fructose using zinc borosilicate (ZBS) activators. Purpose of the research is to study effect of both caramelization and carbonization temperature toward mesopore character and functional group of carbon surface.

EXPERIMENTAL SECTION

Materials

Chemicals used in this study included D-fructose (Merck), $ZnCl_2$ (Merck), HCl 37% (Merck), H_3BO_3 (Merck), and distilled water.

Instrumentation

This research performed some characterizations involving some instruments. Functional groups of the carbons' surface were determined using FTIR spectrophotometer (Shimadzu), Adsorption-desorption nitrogen isotherms of the carbons were measured at the temperature of -196 °C using Surface Area Analyzer (Quantachrome terization) after degassing the carbons at 130 °C for 3 h. Crystal structure of the carbon was determined using X-ray diffractometer (Philip). Pore morphology of the carbon was determined using Transmission Electron Microscope (JEOL/EO). Absorbance of HMF was determined using UV-Vis spectrophotometer (Shimadzu).

Procedure

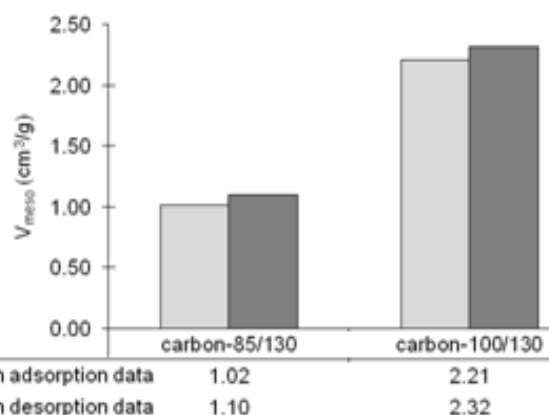#### *Synthesis of carbon at different caramelization temperatures*

A 10 g fructose, 10 g silica gel, 10 g $ZnCl_2$, 12.35 g H_3BO_3, and 60 mL aquadest were placed in a Becker glass and stirred. The mixture then was heated at 85 °C for 6 h, followed by 130 °C for 1 h, and then carbonized under flow of nitrogen gas at 450 °C for 2 h. The carbon-ZBS composite was washed by using HF 48% solution, HCl 1M solution, and aquadest, respectively to remove ZBS from the carbon. The obtained mesoporous carbon then was dried at 130 °C for 6 h and named carbon-85/130. The same procedure was repeated for caramelization temperature of 100 °C for 4 h and the product is named carbon-100/130. The mesoporous carbons were sieved to get of 100–120 mesh particle size. The results were characterized, including pore characteristics and functional group. The crystal structure and pore morphology was conducted for the carbon which has highest mesopore characteristics.

Synthesis of carbon at various carbonization temperatures

The procedure was the same as the procedure for study of caramelization temperature, but it was conducted at caramelization temperature of 100 °C for 4 h and various carbonization temperatures (350, 450, 550, 650, and 750 °C) for 2 h.
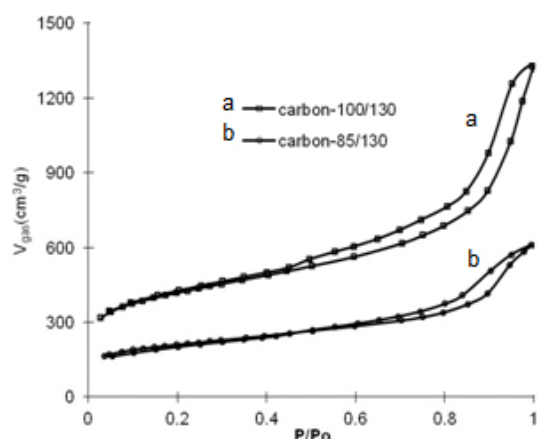
Fig 1. Nitrogen adsorption–desorption isotherm of the carbons synthesized at different caramelization temperatures

Fig 2. Mesopore volume of the carbons synthesized at different caramelization temperatures
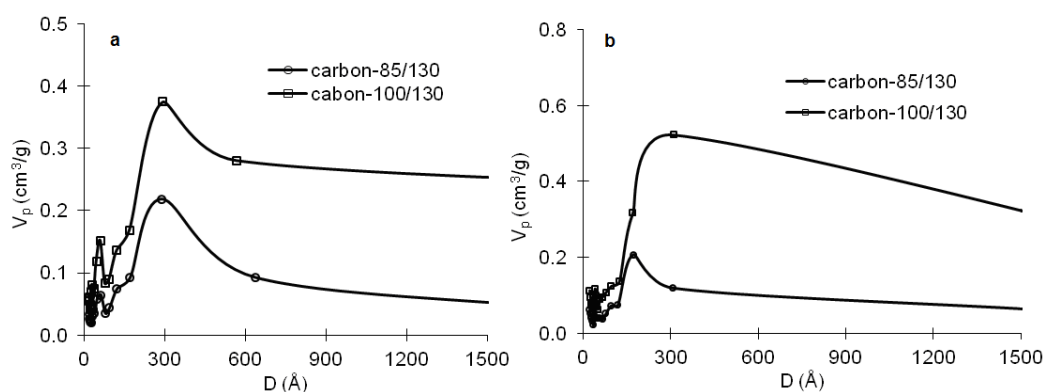
Fig 3. Pore size distribution of the carbons synthesized from fructose with zinc borosilicate and different hydrothermal caramelization temperatures (85 and 100 °C), based on: a) adsorption data, b) desorption data

RESULT AND DISCUSSION

Mesoporous carbons have been synthesized from fructose with ZBS activator at 2 different caramelization temperatures and some various carbonization temperatures. The synthesis involves 2 processes, i.e. caramelization and low temperature carbonization. Pore characterization was conducted with nitrogen adsorption-desorption isotherm at 77 K which was treated using Pierce Orr Dalla Valle (POD) methods [26].

Effect of Caramelization Temperature

Adsorption-desorption isotherm of the carbon is presented in Fig. 1. Isotherm curve gives a rough description about pore characteristics. Fig. 1 shows that both carbons have pattern of type IV isotherm and type I hysteresis, indicating mesopore characteristics and ball pore structure, respectively [26]. Based on data calculation in POD table, mesopore zone stays on range of P/Po 0.15–0.95. Curve slope of the carbon-100/130 is larger than of the carbon-85/130, indicating about larger

mesopore volume, as confirmed later by Fig. 2. Both carbons have inflection point of curve at about P/Po = 0.9. It means that peaks of pore size distribution (PSD) occur at the same pore size which is larger than 100 Å, as confirmed by Fig. 3. The carbon-100/130 has more vertical and longer inflection than the carbon-85/130, indicating the higher peak of PSD, as confirmed by Fig. 4. Based on adsorption-desorption isotherm, it can be concluded roughly that the temperature of 100 °C gives better mesopore quality than 85 °C.

The detail about mesopore volume (V_{meso}) of the carbons is presented in Fig. 2. In Fig. 2, the carbon-100/130 shows higher V_{meso} than the carbon-85/130. This better mesopore quality may be due to improvement of caramelization reaction kinetics by higher temperature [25]. Temperature of 100 °C has higher evaporation kinetics than 85 °C. This condition may create more concentrated HMF which prevent hydrolysis of HMF and creates more caramel product. More caramel amount may produce the thicker pore wall which prevents pore damage in washing process. Mechanism reaction of HMF hydrolysis has been
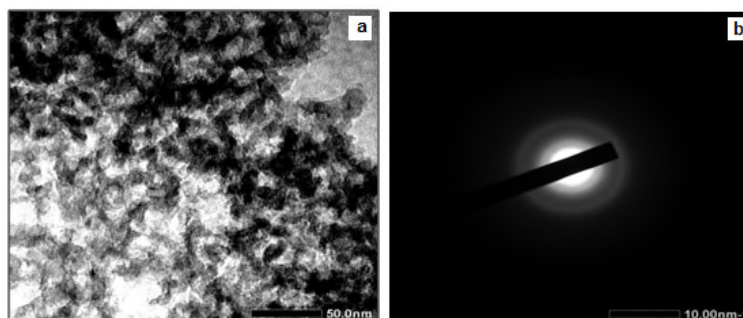
Fig 4. a) TEM image and b) electron diffraction mode of mesoporous carbon from fructose with ZBS activator synthesized at carbonization temperature of 450 °C
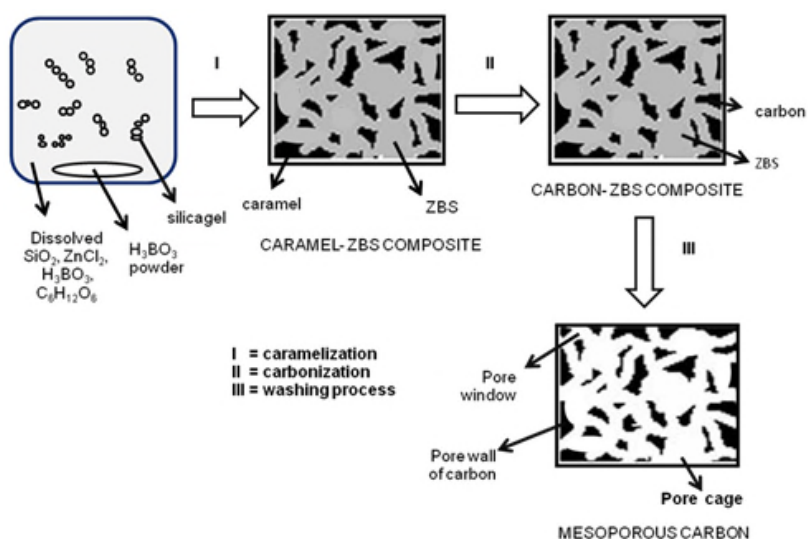
Fig 5. Model of steps in formation of pore structure in synthesis of mesoporous carbon from fructose with ZBS activator as pore template

presented in the previous research [27]. In other hand, the higher temperature creates higher enolisation rate as well as higher proportion of acyclic and furanose form of fructose which improve HMF production [28].

Pore size distributions (PSDs) of the carbons are presented in Fig. 3. The PSD is important to determine pore size uniformity, because peak of PSD describes the largest amount of pore compared to the other pore.

These PSDs are based on POD table by referring to Lowell et al. [26]. Those PSD curves are built based on adsorption data and desorption data because they have correlation with pore cage and pore window, respectively [14]. The PSD curves in Fig. 3 show that the carbon-100/130 has higher peak of PSD than the carbon-85/130, meaning that the former has higher uniformity than the latter. Both carbons have peak of PSD at the same location for pore cage, i.e. at D = 300 Å, but at different locations for pore window, i.e. D = 270 Å for the carbon-100/130 and D = 170 Å for the carbon-85/130. This difference may be due to different pore formation process. Based on visual observation, some silica gel was dissolved by addition of $ZnCl_2$ and some

other was not. It is assumed that pore cage is built by the undissolved silica coated by ZBS network and pore window is built by the dissolved silica reacted with $ZnCl_2$ and H_3BO_3. The undissolved silica particle size may dominate pore size of the pore cage which produce relatively same pore cage. In other hand, the higher caramelization temperature may dissolve more silica to create more ZBS network to create larger size of pore window.

To design model of pore formation by ZBS, morphology of pore is characterized by TEM and presented in Fig. 4. The carbon-100/130 has been chosen for TEM characterization. The carbon in Fig. 4a shows interconnected pore structure (light part). The pore involve pore cage (almost square) and pore window which has long shape like stick and connect the pore cages. The carbon also indicates amorphous pore wall structure (dark part). This amorphous wall is supported by Fig. 4b which shows diffuse electron diffraction mode. Based on pore morphology, visual observation toward dissolution process, and theoretical discussion, the steps of pore formation by ZBS (as pore
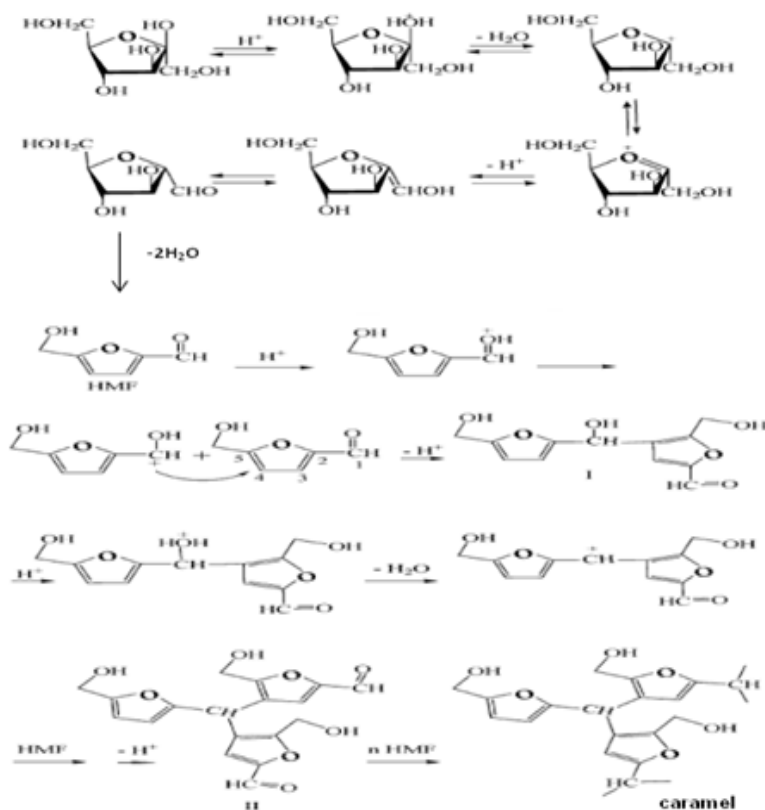
Fig 6. Caramelization mechanism reaction of fructose catalyzed by proton to produce caramel with HMF intermediate [11]
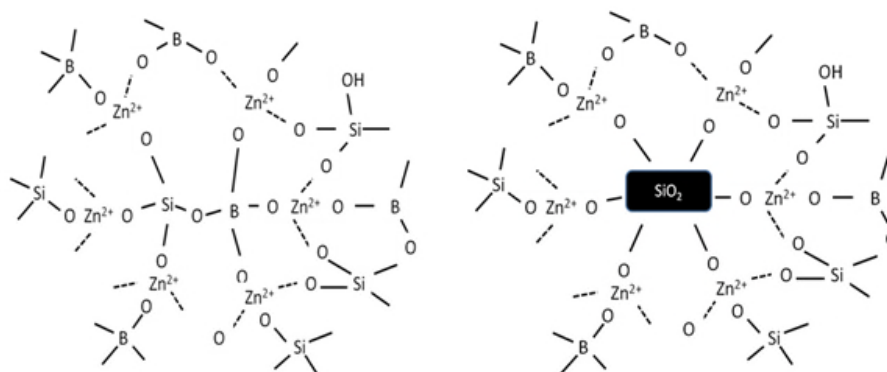
Fig 7. Theoritical chemical structure of ZBS network which builds pore template, involving the undissolved SiO_2 and dissolved silica
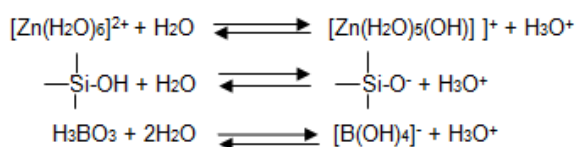

Scheme 1

template) and pore wall formation by fructose are designed in Fig. 5.

Chemically, the steps of synthesis in Fig. 5 involve caramelization reaction of fructose and carbonization

reaction of caramel. There are 2 reactions in the caramelization process, including 1) caramelization reaction of fructose to produce caramel with HMF as intermediate (Fig. 6) and 2) formation of ZBS network by both the dissolved and undissolved silica with $ZnCl_2$, and H_3BO_3 as designed theoretically in Fig. 7, referring to arrangement of BO_4, BO_3, SiO_4, and ZnO_4 polyhedrons in borosilicate glass network [29]. In Fig. 6, the caramelization reaction is catalyzed by proton. Fructose is hydrolyzed to HMF in acid media. Then, HMF is polymerized to caramel by catalization of
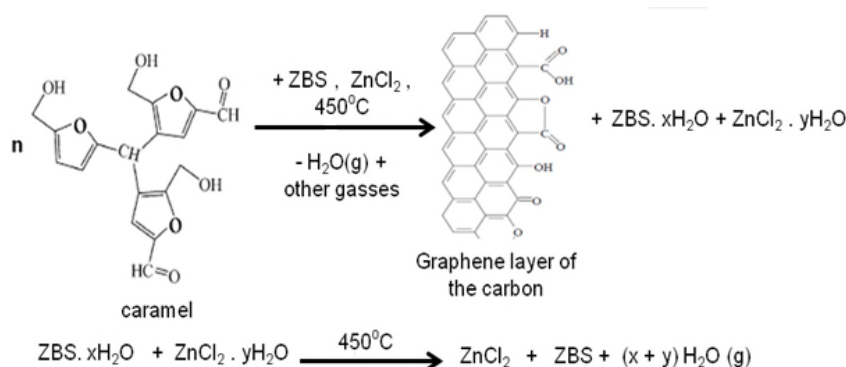
Fig 8. Pyrolysis of caramel with activators of ZBS network and $ZnCl_2$ outside ZBS network in carbonization process at 450 °C
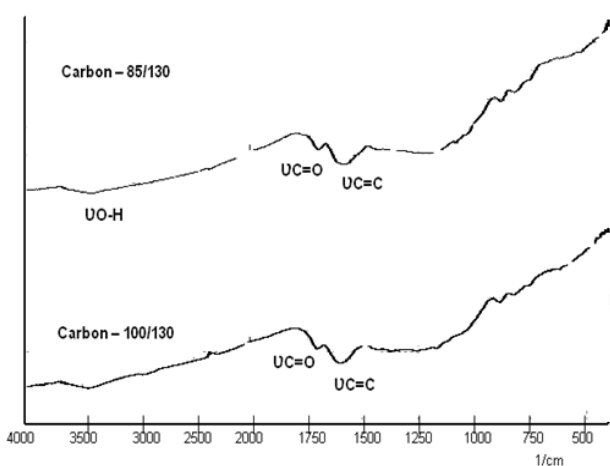
Fig 9. FTIR spectra of mesoporous carbon from fructose with ZBS activator and 2 different caramelization temperatures
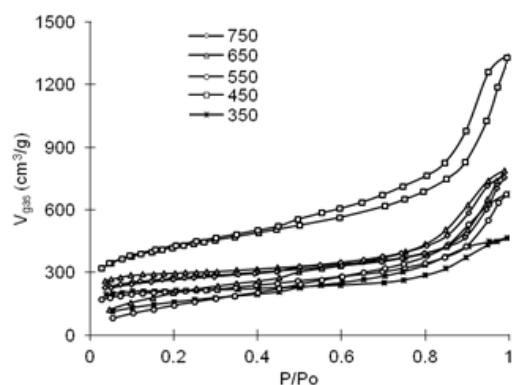
Fig 10. Nitrogen adsorption–desorption isotherm of the carbons synthesized at different carbonization temperatures

acid media too [11]. In this research, the caramelization reaction may be catalyzed by precursors of ZBS ($ZnCl_2$, H_3BO_3, silicagel) because precursors of ZBS, including $ZnCl_2$, H_3BO_3, and silicagel produce proton in water [18-20] (see scheme 1).

The role of ZBS's precursors as catalysts of caramelization reaction is supported by data of HMF (caramel intermediate) absorbance in fructose solution after caramelization reaction in Table 1. In other side, the ZBS network may contain terminal silanol groups (Fig. 7) which can release proton too. The proton can catalyze the caramelization reaction of fructose as described in Fig. 6.

In carbonization process, the caramel is pyrolyzed to produce mesoporous carbon [11], as described in Figure 8. In this process, the remain $ZnCl_2$ which doesn't form ZBS network activates the pyrolysis reaction of caramel. $ZnCl_2$ acts as dehydrating agent which attracts H_2O gas molecules released by decomposition of caramel to form the hydrated compound. This hydrated $ZnCl_2$ finally losses the water molecule by increasing of temperature [30]. This activation can inhibit tar formation and improve carbon yield [10]. The ZBS may also act as dehydrating agent in carbonization process, because the network of ZBS also contains Zn^{2+} cations.

As same as $ZnCl_2$, the Zn^{2+} cations in ZBS attract H_2O molecules to form the hydrated network, and then release them again by increasing of temperature.

The surface functional groups of the carbon is important for catalysis and adsorption applications [31-32]. The functional group is measured with FTIR spectrophotometry and presented in Fig. 9. Spectra of the carbon-85/130 in Fig. 9 shows bands in 1586.34, 1698.21, and 3422.45 cm^{-1}, whereas the carbon-100/130 has bands in 1595.02, 1702.06, and 3401.23 cm^{-1}. Those bands characterize C=C at aromatics rings, C=O, and O-H bonds, respectively [33-35]. The OH bond may be the surface hydroxyl groups and the adsorbed H_2O [36]. The surface hydroxyl may be carboxyl, phenol, or lactol [36]. The C=O bond may be ketone, lactone, or carboxyl [37]. Both carbons have relatively same sharpness of spectra bands, meaning no influence of caramelization temperature toward functional groups of the carbon surface.

Table 1. Absorbance of HMF in fructose solution of 200 g/L after caramelization reaction 100 °C 1 h with different catalyst at mol ratio of catalyst/fructose = 3:1

Catalyst	λ (nm)	Absorbance of HMF
$ZnCl_2$	281.5	0.108
SiO_2	281.5	0.112
H_3BO_3	281.5	0.093
No catalyst	281.5	0.051
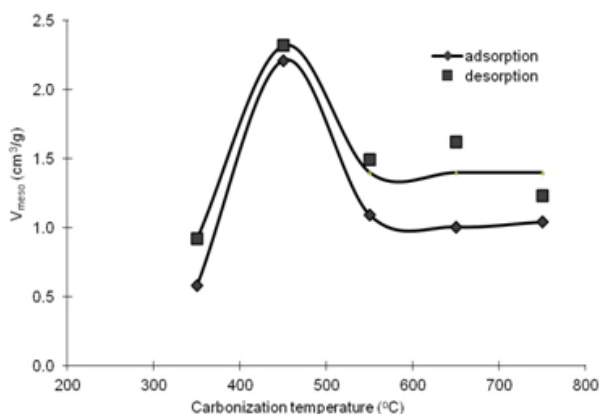
Fig 11. Mesoporous volume of the carbon from fructose using activator of ZBS at various carbonization temperatures
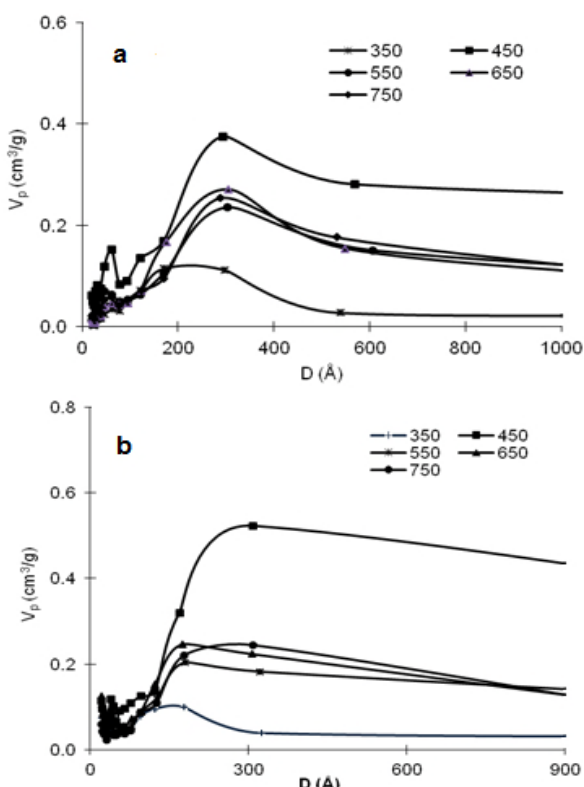

Fig 12. Pore size distribution of mesoporous carbon from fructose and activator of ZBS at various temperatures of carbonization, based on: a) adsorption data, b) desorption data
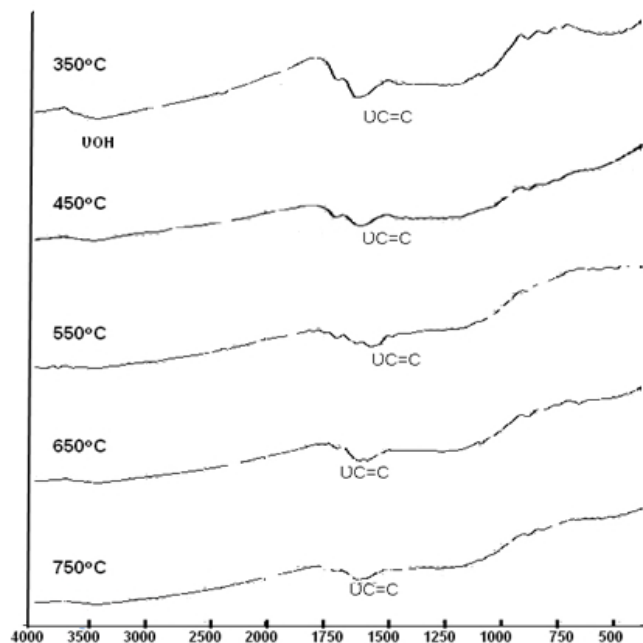
Effect of Carbonization Temperature

The nitrogen adsorption-desorption isotherms of the carbons synthesized at various carbonization temperatures are presented in Fig. 10. All carbons in Fig. 10 exhibit type IV isotherm and type I hysteresis. Those are characteristics of mesopore and ball pore structure [26]. There is increase of curve slope from 350 to 450 °C, especially in the range of P/Po ≥ 0.15, indicating improvement of V_{meso}, as confirmed by Fig. 11. In other side, the slope decreases by increase of temperature from 450 to 550 °C, indicating decrease of V_{meso}, and for range more than 550 °C, the slope is relatively horizontal, indicating the relatively same V_{meso}. All carbons give inflection point of curve at P/Po = 0.9. Based on POD table, it indicates pore distribution peak at pore size > 100 Å, as confirmed by Fig. 12. Curve inflection of the carbon synthesized at 450 °C is much sharper (more vertical) than the others. It indicates higher pore uniformity, as supported by previous research [38-39] and confirmed by Fig. 12. Based on isotherm characterization, it can be concluded roughly that carbonization temperature gives influence toward V_{meso} and uniformity of carbon.

Fig. 11 confirms that V_{meso} of the carbons increase from 350 to 450 °C, decrease from 450 to 550 °C, and relatively constant for range of 550–750 °C, so it means that the optimum temperature occurs at 450 °C. Chemically, improvement of carbonization temperature from 350 to 450 °C probably causes improvement of pyrolysis reaction so that it increases formation of pore wall which improves it's stability in washing process. In other hand, increase of temperature from 450 to 550 °C causes decrease of pore volume. ZBS melt at 500 °C [40]. This melt probably causes rearrangement of ZBS along carbonization which creates more little mesoporous volume. No influence of temperature increase from 550 to 750 °C toward mesoporous volume. This is probably due to relatively same condition of ZBS along carbonization process, i.e. as the melt.

The PSD of the carbons is reported in Fig. 12. The PSD curves in Fig. 12 shows increase of pore uniformity (shown by higher peak) and pore size where uniformity occurs by increase of temperature from 350 to 450 °C. It is probably due to reaction of $ZnCl_2$ and B_2O_3 in melt condition in the 450 °C. $ZnCl_2$ melt at 290 °C [41] and B_2O_3 melt at 450 °C [42]. This reaction potentially improves ZBS particle size which improves pore size of the carbon. In other side, there is decrease of both pore uniformity and pore size by further increase of temperature from 450 to 550 °C, and relatively constant by increase of temperature from 550 to 850 °C. It may be connected to condition of ZBS as melt. The ZBS melt at 500 °C [40]. The melt probably
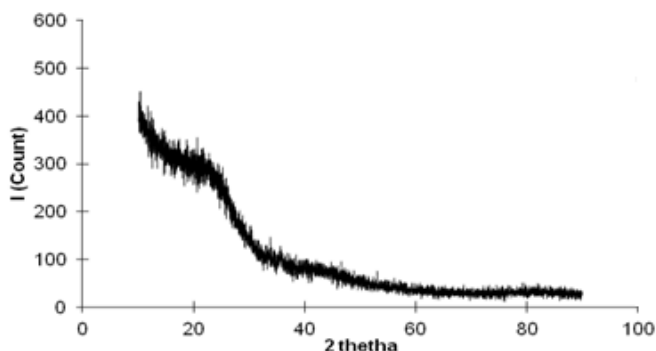
Fig 13. Diffractogram pattern of mesoporous carbon synthesized from fructose with ZBS activator at caramelization temperature of 100 °C and carbonization temperature of 450 °C

Fig 14. FTIR spectra of mesoporous carbon from fructose with ZBS activator at various carbonization temperatures

causes rearrangement of ZBS to form less sized particle which creates less pore size where uniformity of pore occurs with less uniformity. Based on study of the PSD, it is concluded that ZBS improves pore uniformity and pore size where uniformity happened, compared to $ZnCl_2$.

Crystal structure of the carbon synthesized at 450 °C is characterized with X-ray diffraction method and presented in Fig. 13. The diffractogram patterns of the carbons shows broad diffraction peak, indicating content of amorphous structure [10]. There 1 peak at 2θ = 20.74° (d = 4.28 Å). This value is far enough from d value of ideal graphite (d = 3.35 Å) as listed in JCPDS–ICDD card no. 02–0456. Based on calculation by

referring to formula in previous researches [43-44], the carbon has aromaticity fraction 0.68 and degree of graphitization 57%. It means that the carbon contains 44% non graphitic structure.

The functional group was measured with FTIR spectrophotometry and presented in Fig. 14. The spectra in Fig. 14 shows decrease of band sharpness at 1550 cm^{-1} (C=C) by increase of carbonization temperature. The C=C band is connected to vibration of the aromatic structure [33]. This decrease of the functional group of C=C sharpness indicates less polar functional group on graphene layers of the carbon [36]. Fig. 14 also shows decrease of band sharpness at 1650 cm^{-1} (C=O) and 3500 cm^{-1} (OH) with increase of carbonization temperature. The bands of C=O and O-H probably are derived from carboxyl and hydroxyl groups respectively, as reported by previous research [34-35]. Reduction of these functional groups indicates both more complete carbonization reaction and more hydrophobic products by increase of carbonization temperature.

CONCLUSION

In this research, the mesoporous carbons have been synthesized from fructose with ZBS activator at 2 different caramelization temperatures and various carbonization temperatures. Both caramelization and carbonization temperatures give influence toward mesopore quality, but only carbonization temperature gives effect toward functional group of the carbon surface. Increasing of caramelization temperature (85 to 100 °C) and carbonization temperature (350 to 450 °C) improve both V_{meso} and pore uniformity. The highest mesopore quality achieved in this research includes V_{meso} about 2.21 cm^3/g (pore cage) and 2.32 cm^3/g (pore window) with pore uniformity centered at 300 Å (pore cage) and 200 Å (pore window), containing the surface functional groups of C=O and OH, degree of graphitization about 57% and aromaticity fraction about 0.68.

REFERENCES

1. Ryoo, R., Joo, S.H., and Jun, S., 1999, *J. Phys. Chem. B*, 103 (37), 7743–7746.
2. Chi, Y., Geng, W., Zhao, L., Yan, X., Yuan, Q., Li, N., and Li, X., 2012, *J. Colloid Interface Sci.*, 369 (1), 366–372.
3. Lorenc-Grabowska, E., and Gryglewicz, G., 2007, *Dyes Pigm.*, 75 (1), 136–142.
4. Vinu, A., Mori, T., and Ariga, K., 2006, *Sci. Technol. Adv. Mater.*, 7 (8), 753–771.
5. Manabe, T., Ohata, M., Yoshizawa, S., Nakajima, D., Goto, S., Uchida, K., and Yajima, H., 2012,

Effect of Carbonization Temperature, www.geocities.jp/yasizato/Yoshizawa15.pdf, accessed on Nov. 5, 2012

6. Hayashi, J., Kazehaya, A., Muroyama, K., and Watkinson, A.P., 2000, *Carbon*, 38 (13), 1873–1878.
7. Shen, W., Yang, X., Guo, Q., Liu, Y., Song, Y., Han, Z., Sun, Q., and Cheng, J., 2006, *Mater. Lett.*, 60 (29-30), 3517–3521.
8. Lu, A-H., Tüysüs, H., and Schüth, F., 2007, *Microporous Mesoporous Mater.*, 111 (1-3), 117–123.
9. Onal, Y., Akmil-Başar, C., Sarici-Ozdemir, C., and Erdoğan, S, 2006, *J. Hazard Mater.*, 142 (1-2), 138–143.
10. Zhu, Z., Li, A.M., Xia, M., Wan, J., and Zhang, Q., 2008, *Chin. J. Polym. Sci.*, 26 (5), 645−651.
11. Huang, Y., Hu, S., Zuo, S., Xu, Z., Han, C., and Shen, J., 2009, *J. Mater. Chem.,* 19 (11), 7759–7764.
12. Weinbauer, M.G., and Peduzzi, P., 1994, *Mar. Ecol. Prog. Ser.*, 108, 11–20.
13. Hunt, R., 2011, *Virology Chapter Eighteen Hepatitis Viruses*, Microbiology and Immunology On-line, University of South Carolina, http://pathmicro.med.sc.edu/virol/hepatitis-virus.htm, accessed on Dec. 7, 2013.
14. Lee, H.I., Stucky, G.D., Kim, J.H., Pak, C., Chang, H., and Kim, J.M., 2011, *Adv. Mater.*, 23 (20), 2357–2361.
15. Yoon, S.O., Jo, T.H., Kim, K.S., and Kim, S., 2008, *Ceram. Int.*, 34 (8), 2155–2157.
16. Eltepe, H.E., 2004, *The Development of Zinc Borate Production Process*, Dissertation, Chemical Engineering Department, Izmir Institute of Technology, Turkey.
17. Armelao, L., Fabrizio, M., Gialanella, S., and Zordan, F., 2001, *Thin Solid Films*, 394 (1-2), 89–95.
18. Falcone, J., 1982, *ACS Symp. Ser.*, 194, 133–148
19. Shriver, D.F., Atkins, P.W., Langford, C.H., 1990, *Inorganic Chemistry*, Oxford Univ. Press, Oxford.
20. Bowser, J., 1993, *Inorganic Chemistry*, Pubs.co., New York.
21. Seo, J-A., Oh, J., Kim, D.J., Kim, H.K., and Hwang, Y-H., 2004, *J. Non-Cryst. Solids*, 333 (1), 111–114.
22. Zhao, J., Lai, C., Dai, Y., and Xie, J., 2007, *Mater. Lett.*, 61 (23-24), 4639–4642.
23. Rosatella, A.A., Simeonov, S.P., Frade, R.F.M., and Afonso, C.A.M., 2011, *Green Chem.*, 13 (4), 754–793.
24. Chang, W.M., Chen, Y.T., and Shu, C.C., 1998, *Food Preserv.*, 24 (2), 87–93.
25. Quintas, M., Brandão, T.R.S., and Silva, C.L.M., 2007, *J. Food Eng.*, 78 (2), 537–545.
26. Lowell, S., Shield, J.E., Thomas, M.A., and Thommes, M., 2004, *Characterization of Porous Solids and Powders: Surface Area, Pore Size, and Density*, Kluwer Academic Publishers, London, 38–40
27. Girisuta, B., 1975, *Levulinic Acid from Lignocellulosic Biomass* , Thesis, University of Groningen, Groningen
28. Kuster, B.F.M., 1990, *Starch*, 42 (8), 314–321.
29. Calas, G., Grand, M.L., Galoisy, L., and Ghaleb, D., 2003, *J. Nucl. Mater.*, 322 (1), 15–20.
30. Marsh, H., and Reinoso, F.R., 2006, *Activated Carbon*, Elsevier Sci., USA, 331
31. Shen, W., Li, Z., and Liu, Y., 2008, *Recent Pat. Chem. Eng.*, 1 (1), 27–40
32. Nwosu, F.O., Olu-Owolabi, B.I., Adebowale, K.O., Henle, T., and Schwarzenbolz, U., 2009, *Biodivers. Bioavailability*, 3 (2), 89–95.
33. Lua, A.C., and Yang, T., 2005, *J. Colloid Interface Sci.*, 290 (2), 505–513.
34. Chayande, P.K., Singh, S.P., and Yenkie, M.K.N., 2013, *Chem. Sci. Trans.*, 2 (3), 835–840.
35. Allwar, 2012, *Characteristics of Micro- and Mesoporous Structure and Surface Chemistry of Activated Carbons Produced by Oil Palm Shell*, International Conference On Chemical, Ecology and Environmental Sciences (ICEES 2012), Bangkok.
36. Naseh, M.V., Khodadadi, A.A., Mortazavi, Y., Sahraei, O.A., Pourfayaz, F., and Sedghi, S.M., 2009, *World Academy of Science, Engineering and Technology 49*, 3, 134–136.
37. Mahalakshmy, R., Indraneel, P., and Viswanathan, B., 2009, *Indian J. Chem., Sect A*, 48A (3), 352–356.
38. Deng, Y., Liu, C., Yu, T., Liu, F., Zhang, F., Wang, C., Tu, B., Webley, P.A., Wang, H., and Zhao, D., 2007, *Chem. Mater.*, 19 (13), 3271–3277.
39. Cao, Y., Cao, J., Zheng, M., Liu, J., and Ji, G., 2007, *J. Solid State Chem.*, 180 (2), 792–798.
40. Yi, JH., Ko, YN., Koo, HY., Jung, DS., and Kang, YC., 2011, *J.Ceram.Process.Res.,* 12 (2), 122-125
41. Windolz, M., Budavari, S., Blumeti, R.F., and Otterbein, E.S., 1983, *The Merck Index: An Encyclopedia of Chemicals, Drugs, and Biological*, 10th ed., Merck & Co., Inc., USA
42. Sevim, F., Demir, F., Bilen, M., and Okur, H., 2006, *Korean J. Chem. Eng.*, 23 (5), 736–740.
43. Manoj, B., and Kunjomana, A.G., 2012, *Int. J. Electrochem. Sci.*, 7, 3127–3134.
44. Feret, F.R., 1998, *Analyst*, 123 (4), 595–600.